PHYSICS LETTERS B

Observation of the decay $\Lambda_b^0 \to \Lambda_c^+ p\overline{p}\pi^-$

LHCb Collaboration

ABSTRACT

The decay $\Lambda_b^0 \to \Lambda_c^+ p\overline{p}\pi^-$ is observed using pp collision data collected with the LHCb detector at centre-of-mass energies of $\sqrt{s} = 7$ and 8 Tev, corresponding to an integrated luminosity of $3\,\text{fb}^{-1}$. The ratio of branching fractions between $\Lambda_b^0 \to \Lambda_c^+ p\overline{p}\pi^-$ and $\Lambda_b^0 \to \Lambda_c^+ \pi^-$ decays is measured to be

$$\frac{\mathcal{B}(\Lambda_b^0 \to \Lambda_c^+ p\overline{p}\pi^-)}{\mathcal{B}(\Lambda_b^0 \to \Lambda_c^+ \pi^-)} = 0.0540 \pm 0.0023 \pm 0.0032.$$

Two resonant structures are observed in the $\Lambda_c^+ \pi^-$ mass spectrum of the $\Lambda_b^0 \to \Lambda_c^+ p\overline{p}\pi^-$ decays, corresponding to the $\Sigma_c(2455)^0$ and $\Sigma_c^*(2520)^0$ states. The ratios of branching fractions with respect to the decay $\Lambda_b^0 \to \Lambda_c^+ p\overline{p}\pi^-$ are

$$\frac{\mathcal{B}(\Lambda_b^0 \to \Sigma_c^0 p\overline{p}) \times \mathcal{B}(\Sigma_c^0 \to \Lambda_c^+ \pi^-)}{\mathcal{B}(\Lambda_b^0 \to \Lambda_c^+ p\overline{p}\pi^-)} = 0.089 \pm 0.015 \pm 0.006,$$

$$\frac{\mathcal{B}(\Lambda_b^0 \to \Sigma_c^{*0} p\overline{p}) \times \mathcal{B}(\Sigma_c^{*0} \to \Lambda_c^+ \pi^-)}{\mathcal{B}(\Lambda_b^0 \to \Lambda_c^+ p\overline{p}\pi^-)} = 0.119 \pm 0.020 \pm 0.014.$$

In all of the above results, the first uncertainty is statistical and the second is systematic. The phase space is also examined for the presence of dibaryon resonances. No evidence for such resonances is found.

© 2018 The Author(s). Published by Elsevier B.V. This is an open access article under the CC BY license (http://creativecommons.org/licenses/by/4.0/). Funded by SCOAP³.

1. Introduction

The quark model of Gell-Mann [1] and Zweig [2] classifies mesons ($q\overline{q}$) and baryons (qqq) into multiplets, and also allows for hadrons with more than the minimal quark contents. In 2015, LHCb observed two pentaquark states in the decay $\Lambda_b^0 \to J/\psi\, pK^-$ [3]. In the decay channel $\Lambda_b^0 \to \Lambda_c^+ p\overline{p}\pi^-$,[1] charmed dibaryon resonant states could be present. As discussed in Ref. [4], such states could manifest via the decay $\Lambda_b^0 \to \overline{p} + [cd][ud][ud] = \overline{p} + \mathcal{D}_c^+$, where $\mathcal{D}_c^+$ is the dibaryon state with a mass below $4682\,\text{MeV}/c^2$. The subsequent decay of the $\mathcal{D}_c^+$ dibaryon could proceed either via quark rearrangement to the final state $p\Sigma_c^0$, with $\Sigma_c^0 \to \Lambda_c^+ \pi^-$, or via string breaking to the final state $\mathcal{P}_c^0(\overline{u}[cd][ud])$, which could involve a lighter, yet undiscovered $\mathcal{P}_c^0$ pentaquark state, $\mathcal{D}_c^+ \to \mathcal{P}_c^0(\overline{u}[cd][ud])p$, with $\mathcal{P}_c^0 \to \Lambda_c^+ \pi^-$ [4]. The discovery of any of these decay modes would test the predictions of quantum chromodynamics and the fundamental workings of the Standard Model.

In this Letter, the first observation of the decay $\Lambda_b^0 \to \Lambda_c^+ p\overline{p}\pi^-$, referred to as the signal channel, is reported. A measurement is made of its branching fraction relative to the normalisation channel $\Lambda_b^0 \to \Lambda_c^+ \pi^-$. Resonance structures within the $\Lambda_c^+ p\overline{p}\pi^-$ system are also investigated. While no evidence for dibaryon resonances is found, significant contributions from the $\Sigma_c(2455)^0$ and $\Sigma_c^*(2520)^0$ resonances are found in the $\Lambda_c^+ \pi^-$ invariant mass spectrum. The ratios of branching fractions between decays via these resonances, hereinafter denoted as Σ_c^0 and Σ_c^{*0}, and the $\Lambda_c^+ p\overline{p}\pi^-$ inclusive decay are also reported. The measurements in this Letter are based on a data sample of pp collisions collected with the LHCb detector at centre-of-mass energies of $\sqrt{s} = 7$ Tev in 2011 and $\sqrt{s} = 8$ Tev in 2012, corresponding to an integrated luminosity of $3\,\text{fb}^{-1}$.

2. Detector and simulation

The LHCb detector [5,6] is a single-arm forward spectrometer covering the pseudorapidity range $2 < \eta < 5$, designed for the study of particles containing b or c quarks. The detector includes a high-precision tracking system consisting of a silicon-strip ver-

---

[1] Unless explicitly noted, charge conjugate decays are implied.

tex detector surrounding the pp interaction region, a large-area silicon-strip detector located upstream of a dipole magnet with a bending power of about 4 Tm, and three stations of silicon-strip detectors and straw drift tubes placed downstream of the magnet. Different types of charged hadrons are distinguished using information from two ring-imaging Cherenkov (RICH) detectors. Photons, electrons and hadrons are identified by a calorimeter system consisting of scintillating-pad and preshower detectors, an electromagnetic calorimeter and a hadronic calorimeter. Muons are identified by a system composed of alternating layers of iron and multiwire proportional chambers. The online event selection is performed by a trigger [7], which consists of a hardware stage, based on information from the calorimeter and muon systems, followed by a software stage, in which all charged particles with $p_T > 500\,(300)$ MeV/c are reconstructed for 2011 (2012) data, where p_T is the transverse momentum [7]. At the hardware trigger stage, events are required to contain a muon or dimuon pair with high p_T, or a hadron, photon or electron with high transverse energy deposited in the calorimeters. The software trigger requires a two-, three- or four-track secondary vertex with a significant displacement from any primary proton–proton interaction vertices (PVs). At least one charged particle must have a $p_T > 1.7\,(1.6)$ GeV/c for 2011 (2012) data, and be inconsistent with originating from a PV. A multivariate algorithm [8] is used for the identification of secondary vertices consistent with the decay of a b hadron.

Simulated samples of the signal, the normalisation channels and backgrounds produced in pp collisions are generated using PYTHIA [9] with a specific LHCb configuration [10]. Decays of hadronic particles are described by EVTGEN [11], in which final-state radiation is generated using PHOTOS [12]. The interaction of the generated particles with the detector, and its response, are implemented using the GEANT4 toolkit [13] as described in Ref. [14].

3. Candidate selection

The $\Lambda_b^0 \to \Lambda_c^+ p\overline{p}\pi^-$ and $\Lambda_b^0 \to \Lambda_c^+ \pi^-$ candidates are reconstructed using the decay $\Lambda_c^+ \to pK^-\pi^+$. An offline selection is applied, based on a loose preselection, followed by a multivariate analysis. To minimize the systematic uncertainty on the ratio of efficiencies between the signal and the normalisation channels, the selection criteria on the Λ_c^+ candidates are similar between the two channels.

Reconstructed final-state particles in $\Lambda_b^0 \to \Lambda_c^+ p\overline{p}\pi^-$ and $\Lambda_b^0 \to \Lambda_c^+ \pi^-$ candidate decays are required to have a momentum $p > 1$ GeV/c and $p_T > 100$ MeV/c. Protons and antiprotons are required to have $p > 10$ GeV/c to improve particle identification. All final-state particles are also required to be inconsistent with originating from any PV, by rejecting the tracks with a small χ^2_{IP}, where χ^2_{IP} is the difference in the vertex-fit χ^2 of a given PV with or without the track considered, requiring $\chi^2_{IP} > 4$. Candidate Λ_c^+ decays are required to have at least one decay product with $p_T > 500$ MeV/c and $p > 5$ GeV/c, a good vertex-fit quality, and an invariant mass within ± 15 MeV/c^2 of the known Λ_c^+ mass [15]. The scalar sum of the transverse momenta of the Λ_c^+ decay products is required to be greater than 1.8 GeV/c.

The $\Lambda_c^+\pi^-$ candidate is reconstructed by combining a Λ_c^+ candidate with a pion, and the signal candidate is reconstructed by combining a Λ_c^+ candidate with a pion, a proton and an antiproton. These combinations must form a Λ_b^0 candidate with a good-quality vertex and be consistent with originating from the associated PV, defined as that for which the Λ_b^0 candidate has the least χ^2_{IP}. Furthermore, the Λ_c^+ candidate is required to decay downstream of the Λ_b^0 decay vertex. The Λ_b^0 decay time, calculated as

$t = m_{\Lambda_b^0} L/p$, is required to be greater than 0.2 ps, where $m_{\Lambda_b^0}$ is the mass, L is the decay length and p is the momentum of the Λ_b^0 candidate. The Λ_b^0 candidate is also required to have at least one final-state particle in the decay chain with $p_T > 1.7$ GeV/c, $p > 10$ GeV/c, and have at least one track significantly inconsistent with originating from the associated PV by requiring the track to have $\chi^2_{IP} > 16$. Final-state tracks of signal and normalisation channel candidates must pass strict particle-identification requirements based on the RICH detectors, calorimeters and muon stations. A constrained fit [16] is applied to the candidate decay chain for both the signal and the normalisation channels, requiring the Λ_b^0 candidate to come from the associated PV and constraining the Λ_c^+ particle to its known mass [15]. In the case of the search of the resonant contributions, the mass of the Λ_b^0 candidate is also constrained to the known mass [15].

Trigger signals are associated with reconstructed particles from the decays of the signal channel or of the normalisation channel. Selection requirements can therefore be made on the trigger selection itself and on whether the decision was due to the reconstructed candidate decay, other particles produced in the pp collision, or a combination of the two. This association makes it possible to use a data-driven method for the correction and systematic uncertainty estimation on the trigger efficiencies [7]. To take advantage of the similarity between the signal and the normalisation channels, which helps to minimize the systematic uncertainty on the ratio of their efficiencies, candidates are classified in one of the following two hardware trigger categories. In the first category, called Triggered On Signal (TOS), the candidate must include a hadron consistent with originating from the decay of a Λ_c^+ candidate and which deposited enough transverse energy in the calorimeter to satisfy the hardware trigger requirements. The typical value of the transverse energy threshold is around 3.5 GeV/c^2. As the Λ_c^+ baryon is a Λ_b^0 decay product for both the signal and the normalisation channels, this choice minimizes the difference between the Λ_b^0 decay modes. The second category, called Triggered Independent of Signal (TIS), comprises events which satisfied the hardware trigger through signatures unassociated with the complete Λ_b^0 decay chains, either due to a muon with high p_T, or a hadron, photon, or electron with high transverse energy deposited in the calorimeters. The efficiencies of the TIS and TOS requirements are different, so the data are divided into two statistically independent samples, one TIS, and the other TOS and not TIS, which will be referred to as TOS for the rest of this Letter.

The so-called cross-feed backgrounds, contributing under the peak of the invariant mass of the normalisation channel or of the signal channel from the $\overline{B}^0(\overline{B}_s^0) \to D^+(D_s^+)\pi^-$ and $\overline{B}^0(\overline{B}_s^0) \to D^+(D_s^+)p\overline{p}\pi^-$ decays, respectively, with $D^+(D_s^+) \to K^+K^-\pi^+$ or $D^+ \to K^-\pi^+\pi^+$, where either the kaon or pion is misidentified as a proton, are explicitly vetoed when both of the following two conditions are satisfied. First, the mass hypothesis of the proton from the Λ_c^+ candidate is replaced with either the kaon or pion hypothesis, and the resulting invariant mass of the combination is consistent with the known $D^+(D_s^+)$ mass [15] within ± 15 MeV/c^2. Second, the invariant mass of the Λ_c^+ candidate is set to the known $D^+(D_s^+)$ mass [15], and the resulting invariant mass of the Λ_b^0 candidate is consistent with the known $\overline{B}^0(\overline{B}_s^0)$ mass [15] within ± 25 MeV/c^2 for $\Lambda_b^0 \to \Lambda_c^+ p\overline{p}\pi^-$ decays, and within ± 45 MeV/c^2 for $\Lambda_b^0 \to \Lambda_c^+\pi^-$ decays.

Further background reduction is achieved using a multivariate analysis based on a gradient boosted decision tree (BDTG) [17]. The BDTG is trained using twelve variables: the vertex-fit quality of the Λ_c^+ and Λ_b^0 candidates, the decay-vertex displacement along the beamline between the Λ_b^0 and Λ_c^+ candidates, the displacement between the decay vertex of the Λ_b^0 candidate and

the associated PV, the χ^2_{IP} of the Λ_b^0 candidate, the angle between the reconstructed Λ_b^0 momentum and the direction of flight from the associated PV to the decay vertex, the smallest p_T and smallest χ^2_{IP} among the three Λ_c^+ decay products, the p_T and χ^2_{IP} of the pion originating directly from the Λ_b^0 decay, and the smallest p_T and smallest χ^2_{IP} between the p and $\overline{p}$ originating directly from the Λ_b^0 decay. The BDTG training is performed using simulated samples for the signal, and data distributions for the background, with reconstructed invariant mass well above the known Λ_b^0 mass [15]. Cross-feed backgrounds from the decays $\Lambda_b^0 \to \Lambda_c^+ K^+ K^- \pi^-$, $\overline{B}^0 \to \Lambda_c^+ \overline{p} \pi^+ \pi^-$ and $\overline{B}_s^0 \to \Lambda_c^+ \overline{p} K^+ \pi^-$ are explicitly vetoed during the BDTG-training process by requiring the difference between the reconstructed b-hadron mass and its known mass to be greater than $\pm 30\,\mathrm{MeV}/c^2$. The BDTG selection is optimized for the figure of merit $S/\sqrt{S+B}$, where S and B are the expected signal and background yields within $\pm 30\,\mathrm{MeV}/c^2$ of the known Λ_b^0 mass [15]. The initial value of S and B without BDTG selection is obtained from the Λ_b^0 mass spectrum in data. No improvement in the normalisation channel is found using a similar procedure, therefore no BDTG selection is applied. A systematic uncertainty is assessed for this choice in Section 6.

Due to the large number of final-state particles in the Λ_b^0 decays, particles with the same charge may share track segments, representing a possible background. These tracks are referred to as clones, and are suppressed by requiring that the opening angle between any same-charged tracks in the candidate is larger than 0.5 mrad. This selection removes 2% of candidates in the signal sample and 0.1% in the normalisation sample. If multiple Λ_b^0 candidates are reconstructed in one single event, one candidate is chosen at random in the following two cases. First, if the proton from the Λ_c^+ decays is exchanged with that directly from the Λ_b^0 decays, forming two candidates with nearly the same Λ_b^0 mass. Second, if a track from one candidate shares a segment with a track from another candidate. With these criteria, 2.5% of candidates in the signal sample and 0.1% in the normalisation sample are vetoed. After these selections, 0.8% of events in the signal sample and 0.2% in the normalisation sample contain multiple Λ_b^0 candidates. These remaining multiple candidates mainly originate from the random combinations of the final-state tracks, and have a negligible influence on the estimation of the signal yields. No further vetoes on these candidates are applied.

4. Efficiencies

The total efficiencies of the signal and the normalisation decays are given by

$$\epsilon_{\mathrm{total}} = \epsilon_{\mathrm{a}} \cdot \epsilon_{\mathrm{rec\&sel|a}} \cdot \epsilon_{\mathrm{trig|sel}} \cdot \epsilon_{\mathrm{PID}}, \tag{1}$$

where ϵ_{a} represents the geometrical acceptance of the LHCb detector, $\epsilon_{\mathrm{rec\&sel|a}}$ is the efficiency of reconstruction and selection calculated on candidates in the acceptance, $\epsilon_{\mathrm{trig|sel}}$ is the trigger efficiency of the selected candidates, and ϵ_{PID} is the particle-identification efficiency. All efficiencies except ϵ_{PID} and $\epsilon_{\mathrm{trig|sel}}$ are determined from simulation. The particle-identification efficiency is determined from calibration data specific to each data-taking year, binned in momentum and pseudorapidity of the track in question, as well as in the multiplicity of the event [18]. The trigger efficiency is determined from a combination of simulation and data-driven techniques where the agreement between data and simulation is explicitly verified using the normalisation sample satisfying the TIS requirement. All efficiencies are calculated separately for the TIS and TOS trigger samples, and for data-taking year, due to the difference in centre-of-mass energies.

Agreement between data and simulation is improved by applying a per-candidate weight to the p_T and rapidity, y, of the Λ_b^0 baryon in simulated events to match the normalisation sample in the TIS category, which is largely independent of trigger conditions. The p_T and y distributions of Λ_b^0 produced in pp collision are identical for the signal and the normalisation channels, so the same per-candidate weights are applied to the signal sample. The simulated χ^2_{IP} of the final-state particles and the vertex-fit χ^2 of Λ_c^+ candidates are weighted to reproduce the data distributions. The ratio between the efficiencies of the signal and the normalisation channels, ϵ_r, is $(10.00 \pm 0.12)\%$ for the TIS sample and $(11.39 \pm 0.22)\%$ for the TOS sample, including uncertainties due to the limited size of the simulated sample.

5. Fit model and the ratio of branching fractions

The yields in both the signal and the normalisation channels are determined from an unbinned extended maximum-likelihood fit to the corresponding invariant-mass spectra with both the TIS and TOS samples combined. The signal is modelled by a sum of two Crystal Ball functions [19] with a common mean of the Gaussian core, and with the tail parameters fixed from simulation. For both the signal and the normalisation channels, the background from random combinations of final-state particles is described by an exponential function, whose parameters are left free in the fits and are independent between the signal and the normalisation channels. For the normalisation channel, background from the $\Lambda_b^0 \to \Lambda_c^+ \rho^-$ decays, with $\rho^- \to \pi^- \pi^0$ is modelled by the convolution of an empirical threshold function with a Gaussian resolution. The contribution due to misidentification of the kaon to pion from $\Lambda_b^0 \to \Lambda_c^+ K^-$ is modelled by a sum of two Crystal Ball functions. The parameters of these two background sources are taken from simulation. The fits to the invariant-mass distributions for the signal and the normalisation channels are shown in Fig. 1. In this figure, the TIS and TOS samples are combined. From these fits, 926 ± 43 $\Lambda_b^0 \to \Lambda_c^+ p \overline{p} \pi^-$ and $(167.00 \pm 0.50) \times 10^3$ $\Lambda_b^0 \to \Lambda_c^+ \pi^-$ decays are observed.

To determine the ratio of branching fractions $\frac{\mathcal{B}(\Lambda_b^0 \to \Lambda_c^+ p \overline{p} \pi^-)}{\mathcal{B}(\Lambda_b^0 \to \Lambda_c^+ \pi^-)}$, indicated in the following by $\mathcal{B}_r$, a simultaneous fit is performed to the signal and the normalisation channels, each divided into the two independent trigger categories. The yield of the normalisation sample, $N(\Lambda_b^0 \to \Lambda_c^+ \pi^-)$, is a free parameter in the fits, whereas the yield of the signal sample is calculated as $N(\Lambda_b^0 \to \Lambda_c^+ p \overline{p} \pi^-) = \mathcal{B}_r \times \epsilon_r \times N(\Lambda_b^0 \to \Lambda_c^+ \pi^-)$, where ϵ_r is the ratio between the total efficiency of the $\Lambda_b^0 \to \Lambda_c^+ p \overline{p} \pi^-$ and $\Lambda_b^0 \to \Lambda_c^+ \pi^-$ decays. The ratio of branching fractions $\mathcal{B}_r$ is the same for the TIS and TOS subsamples and is measured to be $\mathcal{B}_r = 0.0542 \pm 0.0023$. The corresponding signal yields are 677 ± 29 for the TIS subsample and 259 ± 11 for the TOS subsample; the yields in the normalisation sample are $(124.9 \pm 0.4) \times 10^3$ for the TIS subsample and $(41.9 \pm 0.2) \times 10^3$ for the TOS subsample.

6. Systematic uncertainties

The systematic uncertainties on the measurement of the ratio of branching fractions are listed in Table 1. The total systematic uncertainty is determined from the sum in quadrature of all terms.

First, the uncertainty related to the background modelling is considered. In the signal sample, the exponential function is replaced with a second-order polynomial for the background component. For the normalisation channel, the model is varied by using the sum of two exponential functions. The resulting uncertainty on the ratio of branching fractions is 0.6%. The uncertainties due to the $\Lambda_b^0 \to \Lambda_c^+ K^-$ shape parameters are assessed by increasing the
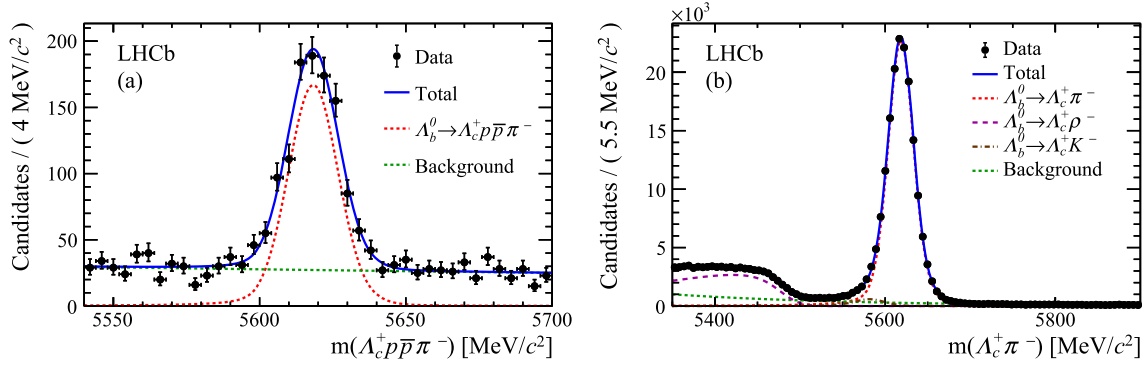
Fig. 1. Invariant mass distributions of the (a) $\Lambda_b^0 \to \Lambda_c^+ p\overline{p}\pi^-$ and (b) $\Lambda_b^0 \to \Lambda_c^+ \pi^-$ candidates. Fit results are overlaid as a solid blue line. For (a), the red dotted line represents the signal component and the green dotted line the background due to random combinations. For (b), the red dotted line is the signal component, the green dotted line is the random combination background, the purple dashed line is the contribution from $\Lambda_b^0 \to \Lambda_c^+ \rho^-$ and the brown dashed–dotted line represents the contribution from $\Lambda_b^0 \to \Lambda_c^+ K^-$. (For interpretation of the colours in the figure(s), the reader is referred to the web version of this article.)

Table 1
Summary of systematic uncertainties and correction factors to the ratio of branching fractions measurement. All uncertainties are given as a percentage of the ratio of branching fractions.

Source	Uncertainty (%)	Correction factor
Background fit model	0.7	–
Signal fit model	0.1	–
PID efficiency	0.3	–
Tracking efficiency calibration	0.8	0.985
Kinematic range of final-state tracks	0.7	–
Hadron interaction	4.4	–
p_T, y weighting	1.0	–
Trigger efficiency	2.9	–
Simulated sample size	1.3	–
Candidates with clone tracks and multiple candidates	0.2	–
Veto of the reflection background	0.4	–
Λ_c^+ Dalitz weighting	0.2	0.984
Λ_c^+ polarization	0.3	0.987
Resonant structures	1.8	1.041
Total	6.0	0.996

width of the Crystal Ball functions by 10%, corresponding to two standard deviations, resulting in a change of 0.1%. The uncertainty due to the $\Lambda_b^0 \to \Lambda_c^+ \rho^-$ contribution is estimated by varying the shape parameters by one standard deviation, resulting in an uncertainty of 0.4%. The total uncertainty on the ratio of the branching fractions due to the background modelling is 0.7%.

The signal-model parameterization is changed to a single Hypatia function [20], where the mean and width are allowed to float and all other parameters are taken from simulation, resulting in an uncertainty of 0.1%.

The uncertainty on the relative efficiency of the particle identification is assessed by generating pseudoexperiments. For each pseudoexperiment, efficiencies in different momentum, pseudorapidity and multiplicity bins are determined from independent Gaussian distributions with mean values equal to the nominal efficiencies and widths corresponding to their uncertainties. This procedure is repeated 1000 times, and the width of the resulting efficiency is taken as the systematic uncertainty. This procedure, performed separately for the TIS and TOS samples, results in a 0.13% uncertainty for both samples. Binning effects on the efficiency are estimated by halving the bin size of the momentum distributions, resulting in a relative change of 0.2% for the TIS sample and 0.1% for the TOS sample. The total uncertainty on the relative efficiency for the TIS and TOS samples is 0.24% and 0.16%, respectively, corresponding to an uncertainty of 0.3% on the ratio of the branching fractions.

Tracking efficiencies are determined with simulated events weighted to match the kinematic properties of dedicated calibration samples. The weights are determined as a function of the kinematic variables, separately for each data-taking year [21]. The kinematic properties of the Λ_c^+ decay products are similar for the signal and the normalisation samples and therefore provide minor contributions to the total tracking efficiency ratio. The dominant contribution to the systematic uncertainty comes from the knowledge of the p and $\overline{p}$ tracking efficiencies, whose systematic uncertainties are fully correlated. The efficiency correction procedure gives a change in efficiency of 2.0% for the TIS sample and 1.4% for the TOS sample, yielding a total correction factor of 0.985 for the ratio of branching fractions, and a systematic uncertainty of 0.4% for each of the p and $\overline{p}$ mainly stemming from the finite size of the calibration sample [21].

Due to distinct trigger requirements, the kinematic acceptance of the calibration samples differs slightly from the signal and the normalisation channels. A nonnegligible fraction of candidates have final-state particles in a kinematic range outside of the regions covered by the calibration samples. About 20% of the candidates from both channels fall in this category due to the low-momentum pion from the Λ_c^+ decay. In addition, 10% of the candidates from the signal channel are also affected, mainly due to the pion originating from the Λ_b^0 decay. For all of these outside-range candidates, the efficiency correction in the nearest available bin is used. As the effects for Λ_c^+ decays cancel in the relative efficiency, only the additional 10% candidates in the signal channel contribute a 0.7% uncertainty on the relative efficiency.

Hadronic interactions with the LHCb detector contribute an additional uncertainty of 2.2% on the ratio of the branching fractions

for each p or $\overline{p}$ (4.4% in total), which is obtained from simulation, accounting for the imperfect knowledge of material budget of the LHCb detector [22].

Per-candidate weights depending on p_T and y of the Λ_b^0 baryon are applied in simulated events to improve the agreements between data and simulation. Systematic uncertainties for the weighting due to the finite size of the normalisation sample are assessed with pseudoexperiments. In each pseudoexperiment, the weights are varied within their uncertainties, and the results are propagated to the ratio of branching fractions. The standard deviation of the obtained distributions is taken as a systematic uncertainty, resulting in 0.65% for the TIS sample and 0.65% for the TOS sample. The systematic uncertainties due to the binning scheme of the weighting in p_T and y are estimated by halving the bin size, or using the gradient boosting [23] [24], which is an unbinned method of weighting, to check the changes on the relative efficiencies. The resulting systematic uncertainties are 0.43% for the TIS sample and 1.5% for the TOS sample. After propagation through the entire fit procedure, this results in an uncertainty of 1.0% on the ratio of the branching fractions.

Trigger efficiencies for the TOS samples are also assessed using pseudoexperiments which are propagated to the final measurement, resulting in a final uncertainty of 0.1%. The trigger efficiency of the TIS sample is taken from simulation. Its systematic uncertainty is computed from the difference between the TIS efficiency taken from data and simulation for events which are triggered both on the Λ_c^+ candidate and also on other tracks unassociated to the signal decay. As a result, a systematic uncertainty of 3.9% is assigned for the relative trigger efficiency of the TIS sample, corresponding to an uncertainty of 2.9% on the ratio of the branching fractions.

The effect of the finite size of the simulated samples is assessed by considering the possible variation of the efficiency with weighted samples in a bin of p_T and rapidity of the Λ_b^0 candidate, and the corresponding systematic uncertainty on the efficiency of the signal or normalisation channel, TIS or TOS sample, is given by

$$\sigma_\epsilon = \sqrt{\sum_i \epsilon_i(1-\epsilon_i)N_i w_i} \Big/ \sum_i N_i w_i, \qquad (2)$$

where for each bin i, N_i is the number of candidates, w_i is the single event weight, and ϵ_i is the single event efficiency. The total uncertainty on the relative efficiency for the TIS and TOS samples is 1.2% and 1.9%, respectively, corresponding to an uncertainty of 1.3% on the ratio of the branching fractions.

The uncertainty due to the removal of candidates reconstructed with clone tracks and multiple candidates is assessed by applying the same procedure to simulation, resulting in a difference of 0.2%.

Vetoes on the invariant mass of possible cross-feed backgrounds may bias the signal mass distributions. An uncertainty of 0.4% is determined by changing the fit range of the normalisation sample to begin at 5450 MeV/c^2, instead of 5350 MeV/c^2.

The agreement between data and simulation in the $\Lambda_c^+ \to pK^-\pi^+$ decay is also tested by comparing the Dalitz plot distributions. The normalisation sample is weighted in the $m^2(pK^-)$ versus $m^2(K^-\pi^+)$ plane. Due to the smaller sample size of the signal channel, weights obtained from the normalisation channel are applied to the signal. The resulting procedure renders all distributions consistent within one statistical standard deviation. The difference in the ratio of branching fractions is 1.3% smaller than the nominal result, providing a correction factor of 0.984. An uncertainty of 0.2% is determined by using an alternative binning scheme and varying the Dalitz-plot weights by their statistical uncertainties.

The polarization of the Λ_b^0 particles has been measured to be consistent with zero [25], but the weak decay of the Λ_b^0 baryon may induce a polarization in the Λ_c^+ system. In the simulation, it is assumed that the Λ_c^+ particle is unpolarized, leading to a difference in angular distributions between simulation and data. A possible effect due to the Λ_c^+ polarization is assessed by applying a weighting procedure to the distribution of the Λ_c^+ helicity angle, which is defined as the angle between the Λ_c^+ flight direction in the Λ_b^0 rest frame and the direction of the pK^- pair in the Λ_c^+ rest frame. This weight is obtained through a comparison between the angular distributions in simulation and data for the signal and the normalisation channels individually. Applying this weight to both the signal and the normalisation channels does not change the efficiency with respect to any of the other possible angles, and leads to a change of 1.1% in the relative efficiency for the TOS sample and 1.4% for the TIS sample. Propagation of these uncertainties leads to a correction factor of 0.987 on the ratio of the branching fractions. An uncertainty of 0.3% is determined by using an alternative binning scheme and varying the single-candidate weights by their statistical uncertainties.

Simulated data are generated using a phase-space model for the Λ_b^0 decay, which does not take into account possible resonances in the $\Lambda_c^+ p\overline{p}\pi^-$ system. Upon inspection, clear signals from the Σ_c^0 and Σ_c^{*0} resonances are found, as described in Section 7. To assess the effect of these resonances, the simulation is weighted to reproduce the data. Weights are applied in two invariant mass dimensions, namely the $\Lambda_c^+\pi^-$ invariant mass and another invariant mass of any two or three body combination. Among these weighting strategies, applying weights in $m(\Lambda_c^+\pi^-)$ and $m(p\pi^-)$ (option 1) leads to the smallest $\mathcal{B}_r$, while weights in $m(\Lambda_c^+\pi^-)$ and $m(p\overline{p}\pi^-)$ (option 2) leads to the largest $\mathcal{B}_r$. A correction factor is computed as the average of the central values of the ratio of branching fractions for the two options divided by the nominal branching fraction, with an uncertainty determined by half the difference between the two ratios of branching fractions. This leads to a correction factor of 1.041 and a resulting systematic uncertainty of 1.8%.

Uncertainties due to the use of the BDTG are tested by repeating the BDTG training and selection procedure to the normalisation channel without variables related to the $p\overline{p}$ pair; the ratio of branching fractions is found to be consistent.

7. Resonance structures in the $\Lambda_c^+\pi^-$ mass spectrum

As the resonant structure of $\Lambda_b^0 \to \Lambda_c^+ p\overline{p}\pi^-$ decays is unexplored, the resonances in the $\Lambda_c^+\pi^-$ system are studied. An unbinned maximum-likelihood fit of the $\Lambda_c^+\pi^-$ mass is performed for those candidates which pass all the selection criteria for the signal $\Lambda_b^0 \to \Lambda_c^+ p\overline{p}\pi^-$ decays, to determine if there are resonant contributions. In this case the Λ_b^0 candidate is constrained to its known mass [15] when obtaining the $\Lambda_c^+\pi^-$ invariant mass spectrum.

The signal shapes of the Σ_c^0 and Σ_c^{*0} resonances are given as the modulus squared of the relativistic Breit–Wigner function [15],

$$|\text{BW}(m|M_0, \Gamma_0)|^2 = \left| 1/(M_0^2 - m^2 - iM_0\Gamma(m)) \right|^2, \qquad (3)$$

multiplied by $m\Gamma(m)$, and convolved with a Gaussian resolution determined from simulation. Here, M_0 is the known value of the Σ_c^0 or Σ_c^{*0} mass [15], m is the $\Lambda_c^+\pi^-$ invariant mass, and Γ_0 is the mass-independent width of the resonance, namely 1.83 MeV/c^2 for the Σ_c^0 and 15.3 MeV/c^2 for the Σ_c^{*0} resonance. The mass-dependent width is given by

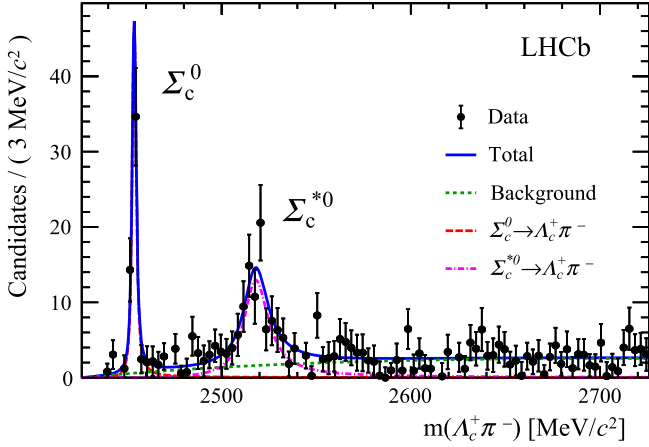**Fig. 2.** Invariant mass of the $\Lambda_c^+\pi^-$ system from the decay $\Lambda_b^0 \to \Lambda_c^+ p\overline{p}\pi^-$. The Σ_c^0 and Σ_c^{*0} resonances are indicated. The fit to the data is shown as a blue continuous line, with the background component shown as a green dotted line, the Σ_c^0 shape shown as a dashed red line, and the Σ_c^{*0} shape shown as a dash-dotted magenta line.

$$\Gamma(m) = \Gamma_0 \times \left(\frac{q}{q_0}\right)^{2L+1} \frac{M_0}{m} B_L(q, q_0, d)^2, \qquad (4)$$

where L is the angular momentum in the resonance decay, q is the momentum of the Λ_c^+ baryon in the $\Sigma_c^{(*)0}$ rest frame, $q_0 \equiv q(m = M_0)$ and d stands for the size of the $\Sigma_c^{(*)0}$ particles. From parity and angular momentum conservation, it follows that $L = 1$. The width also depends on the Blatt–Weisskopf factor $B_L(q, q_0, d)$ [26], where the value of d is set to be 1 fm (5 GeV^{-1} in natural units). The ratio of widths of the Gaussian resolution functions for the Σ_c^0 and Σ_c^{*0} resonances is fixed from simulation to be 1.96. The background is described with an empirical threshold function. The fit shown in Fig. 2 yields 59 ± 10 $\Lambda_b^0 \to \Sigma_c^0 p\overline{p}$ decays and 104 ± 17 $\Lambda_b^0 \to \Sigma_c^{*0} p\overline{p}$ decays.

The relative efficiencies for the decays $\Lambda_b^0 \to \Sigma_c^0 p\overline{p}$, with $\Sigma_c^0 \to \Lambda_c^+\pi^-$ and $\Lambda_b^0 \to \Sigma_c^{*0} p\overline{p}$, with $\Sigma_c^{*0} \to \Lambda_c^+\pi^-$ with respect to $\Lambda_b^0 \to \Lambda_c^+ p\overline{p}\pi^-$ decays are determined with an analogous procedure as that for the $\Lambda_b^0 \to \Lambda_c^+ p\overline{p}\pi^-$ decays relative to the $\Lambda_b^0 \to \Lambda_c^+\pi^-$ decays, but with the trigger samples combined due to limited sample size. The efficiencies are 0.685 ± 0.021 for the Σ_c^0 mode and 0.904 ± 0.021 for the Σ_c^{*0} mode, relative to $\Lambda_b^0 \to \Lambda_c^+ p\overline{p}\pi^-$.

Many of the systematic uncertainties cancel out in the measurement of the ratio of branching fractions, with the remaining systematic uncertainties stemming from the yield determination. The value of d in the Blatt–Weisskopf factor is varied between 1.5 and 0.5 fm, with the largest variation for each resonance taken as the systematic uncertainty, resulting in 3.4% for the Σ_c^0 resonance and 1.9% for the Σ_c^{*0} resonance. The background shape is changed to a third-order polynomial, with a relative difference of 1.7% for the Σ_c^0 resonance and 10.6% for the Σ_c^{*0} resonance taken as the systematic uncertainty. The masses and widths of the $\Sigma_c^{(*)0}$ resonances are allowed to float within one standard deviation of their known values [15], resulting in a 3.8% difference of the raw yield for the Σ_c^0 resonance and 2.2% difference for the Σ_c^{*0} resonance. All uncertainties in the relative efficiency cancel, except for those related to the weighting due to resonant structures in the $\Lambda_c^+\pi^-$ system. The scaling factor of 1.041, with an uncertainty of 1.8% on the relative efficiency, which is shown in Table 1, is therefore used here as well. The resulting ratios of branching fractions are

$$\frac{\mathcal{B}(\Lambda_b^0 \to \Sigma_c^0 p\overline{p}) \times \mathcal{B}(\Sigma_c^0 \to \Lambda_c^+\pi^-)}{\mathcal{B}(\Lambda_b^0 \to \Lambda_c^+ p\overline{p}\pi^-)} = 0.089 \pm 0.015 \pm 0.006,$$

$$\frac{\mathcal{B}(\Lambda_b^0 \to \Sigma_c^{*0} p\overline{p}) \times \mathcal{B}(\Sigma_c^{*0} \to \Lambda_c^+\pi^-)}{\mathcal{B}(\Lambda_b^0 \to \Lambda_c^+ p\overline{p}\pi^-)} = 0.119 \pm 0.020 \pm 0.014,$$

where the first uncertainty is statistical and the second is systematic.

8. Search for dibaryon resonances

The existence of dibaryon resonances, $\mathscr{D}_c^+ \to p\Sigma_c^0$, is investigated in the $\Lambda_c^+\pi^- p$ mass spectrum of background-subtracted data. The full $m(\Lambda_c^+\pi^-)$ spectrum is considered, while the signal regions of Σ_c^0 and Σ_c^{*0} resonances are defined by the ranges $2450 < m(\Lambda_c^+\pi^-) < 2458$ MeV/c^2 and $2488 < m(\Lambda_c^+\pi^-) < 2549$ MeV/c^2, respectively. The background is subtracted with the *sPlot* technique [27]. No peaking structures are observed in the distributions shown in Fig. 3. The two-dimensional distribution of $m(\Lambda_c^+ p\pi^-)$ versus $m(\Lambda_c^+\pi^-)$ has been checked and does not exhibit any clear structure.

9. Conclusion

The first observation of the decay $\Lambda_b^0 \to \Lambda_c^+ p\overline{p}\pi^-$ is presented. The ratio of the branching fractions using the decay $\Lambda_b^0 \to \Lambda_c^+\pi^-$ as the normalisation channel is measured to be

$$\frac{\mathcal{B}(\Lambda_b^0 \to \Lambda_c^+ p\overline{p}\pi^-)}{\mathcal{B}(\Lambda_b^0 \to \Lambda_c^+\pi^-)} = 0.0540 \pm 0.0023 \pm 0.0032,$$

using data corresponding to an integrated luminosity of 3 fb^{-1} collected during 2011 and 2012 with the LHCb detector. Contributions from the $\Sigma_c(2455)^0$ and $\Sigma_c^*(2520)^0$ resonances are observed, and the ratios of their branching fractions with respect to the $\Lambda_b^0 \to \Lambda_c^+ p\overline{p}\pi^-$ decays are measured to be

$$\frac{\mathcal{B}(\Lambda_b^0 \to \Sigma_c^0 p\overline{p}) \times \mathcal{B}(\Sigma_c^0 \to \Lambda_c^+\pi^-)}{\mathcal{B}(\Lambda_b^0 \to \Lambda_c^+ p\overline{p}\pi^-)} = 0.089 \pm 0.015 \pm 0.006,$$

$$\frac{\mathcal{B}(\Lambda_b^0 \to \Sigma_c^{*0} p\overline{p}) \times \mathcal{B}(\Sigma_c^{*0} \to \Lambda_c^+\pi^-)}{\mathcal{B}(\Lambda_b^0 \to \Lambda_c^+ p\overline{p}\pi^-)} = 0.119 \pm 0.020 \pm 0.014.$$

In all of the above results, the first uncertainty is statistical and the second is systematic.

The mass spectra of the $\Lambda_c^+ p\pi^-$ final state are also inspected for possible dibaryon resonances, but no evidence of peaking structures is observed.
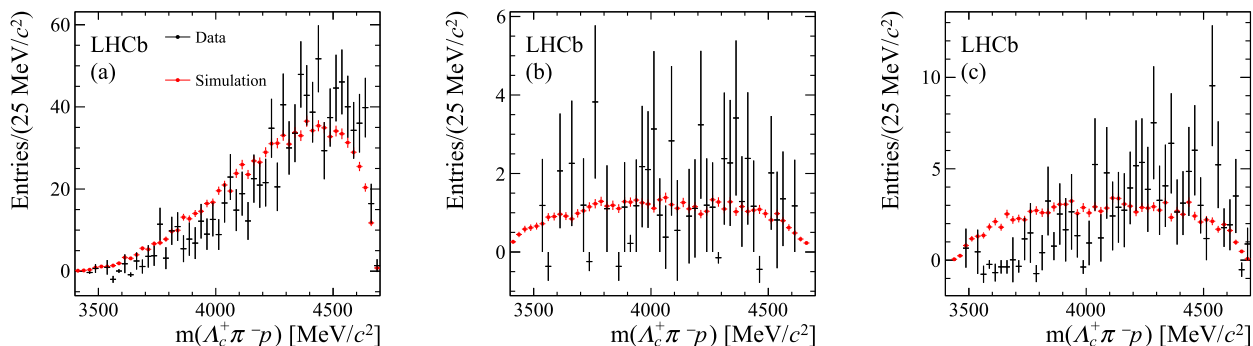
Fig. 3. Background-subtracted mass spectrum of the $\Lambda_c^+\pi^-p$ system from the decay $\Lambda_b^0 \to \Lambda_c^+ p\overline{p}\pi^-$ in (a) the full $\Lambda_c^+\pi^-$ mass spectrum, (b) the signal region of the Σ_c^0 resonance, and (c) the signal region of the Σ_c^{*0} resonance. In all figures, the black points are data and the red points are simulated events where the Λ_b^0 baryon decays to the $\Lambda_c^+ p\overline{p}\pi^-$ final state (a) based on a uniform-phase-space model, (b) through the Σ_c^0 resonance and (c) through the Σ_c^{*0} resonance. No evident peaking shapes are visible.

References

[1] M. Gell-Mann, A schematic model of baryons and mesons, Phys. Lett. 8 (1964) 214.

[2] G. Zweig, An SU_3 model for strong interaction symmetry and its breaking, CERN-TH-401, 1964.

[3] LHCb Collaboration, R. Aaij, et al., Observation of $J/\psi\,p$ resonances consistent with pentaquark states in $\Lambda_b^0 \to J/\psi\,pK^-$ decays, Phys. Rev. Lett. 115 (2015) 072001, arXiv:1507.03414.

[4] L. Maiani, A.D. Polosa, V. Riquer, From pentaquarks to dibaryons in $\Lambda_b^0(5620)$ decays, Phys. Lett. B 750 (2015) 37, arXiv:1508.04459.

[5] LHCb Collaboration, A.A. Alves Jr., et al., The LHCb detector at the LHC, J. Instrum. 3 (2008) S08005.

[6] LHCb Collaboration, R. Aaij, et al., LHCb detector performance, Int. J. Mod. Phys. A 30 (2015) 1530022, arXiv:1412.6352.

[7] R. Aaij, et al., The LHCb trigger and its performance in 2011, J. Instrum. 8 (2013) P04022, arXiv:1211.3055.

[8] V.V. Gligorov, M. Williams, Efficient, reliable and fast high-level triggering using a bonsai boosted decision tree, J. Instrum. 8 (2013) P02013, arXiv:1210.6861.

[9] T. Sjöstrand, S. Mrenna, P. Skands, A brief introduction to PYTHIA 8.1, Comput. Phys. Commun. 178 (2008) 852, arXiv:0710.3820;
T. Sjöstrand, S. Mrenna, P. Skands, PYTHIA 6.4 physics and manual, J. High Energy Phys. 05 (2006) 026, arXiv:hep-ph/0603175.

[10] I. Belyaev, et al., Handling of the generation of primary events in Gauss, the LHCb simulation framework, J. Phys. Conf. Ser. 331 (2011) 032047.

[11] D.J. Lange, The EvtGen particle decay simulation package, Nucl. Instrum. Methods A 462 (2001) 152.

[12] P. Golonka, Z. Was, PHOTOS Monte Carlo: a precision tool for QED corrections in Z and W decays, Eur. Phys. J. C 45 (2006) 97, arXiv:hep-ph/0506026.

[13] Geant4 Collaboration, J. Allison, et al., Geant4 developments and applications, IEEE Trans. Nucl. Sci. 53 (2006) 270;
Geant4 Collaboration, S. Agostinelli, et al., Geant4: a simulation toolkit, Nucl. Instrum. Methods A 506 (2003) 250.

[14] M. Clemencic, et al., The LHCb simulation application, Gauss: design, evolution and experience, J. Phys. Conf. Ser. 331 (2011) 032023.

[15] Particle Data Group, C. Patrignani, et al., Review of particle physics, Chin. Phys. C 40 (2016) 100001.

[16] W.D. Hulsbergen, Decay chain fitting with a Kalman filter, Nucl. Instrum. Methods A 552 (2005) 566, arXiv:physics/0503191.

[17] L. Breiman, J.H. Friedman, R.A. Olshen, C.J. Stone, Classification and Regression Trees, Wadsworth International Group, Belmont, California, USA, 1984.

[18] A. Powell, et al., Particle identification at LHCb, PoS ICHEP2010 (2010) 020, LHCb-PROC-2011-008.

[19] T. Skwarnicki, A Study of the Radiative Cascade Transitions Between the Upsilon-Prime and Upsilon Resonances, PhD thesis, Institute of Nuclear Physics, Krakow, 1986, DESY-F31-86-02.

[20] D. Martínez Santos, F. Dupertuis, Mass distributions marginalized over per-event errors, Nucl. Instrum. Methods A 764 (2014) 150, arXiv:1312.5000.

[21] LHCb Collaboration, R. Aaij, et al., Measurement of the track reconstruction efficiency at LHCb, J. Instrum. 10 (2015) P02007, arXiv:1408.1251.

[22] R. Aaij, et al., Performance of the LHCb vertex locator, J. Instrum. 9 (2014) 09007, arXiv:1405.7808.

[23] J.H. Friedman, Greedy function approximation: a gradient boosting machine, Ann. Stat. (2001) 1189.

[24] S. Belov, L. Dudko, D. Kekelidze, A. Sherstnev, HepML, an XML-based format for describing simulated data in high energy physics, Comput. Phys. Commun. 181 (2010) 1758, arXiv:1001.2576.

[25] LHCb Collaboration, R. Aaij, et al., Measurements of the $\Lambda_b^0 \to J/\psi\,\Lambda$ decay amplitudes and the Λ_b^0 polarisation in pp collisions at $\sqrt{s} = 7$ Tev, Phys. Lett. B 724 (2013) 27, arXiv:1302.5578.

[26] F. Von Hippel, C. Quigg, Centrifugal-barrier effects in resonance partial decay widths, shapes, and production amplitudes, Phys. Rev. D 5 (1972) 624.

[27] M. Pivk, F.R. Le Diberder, sPlot: a statistical tool to unfold data distributions, Nucl. Instrum. Methods A 555 (2005) 356, arXiv:physics/0402083.

LHCb Collaboration

R. Aaij [43], B. Adeva [39], M. Adinolfi [48], Z. Ajaltouni [5], S. Akar [59], P. Albicocco [19], J. Albrecht [10], F. Alessio [40], M. Alexander [53], A. Alfonso Albero [38], S. Ali [43], G. Alkhazov [31], P. Alvarez Cartelle [55], A.A. Alves Jr [59], S. Amato [2], S. Amerio [23], Y. Amhis [7], L. An [3], L. Anderlini [18], G. Andreassi [41], M. Andreotti [17,g], J.E. Andrews [60], R.B. Appleby [56], F. Archilli [43], P. d'Argent [12], J. Arnau Romeu [6], A. Artamonov [37], M. Artuso [61], E. Aslanides [6], M. Atzeni [42], G. Auriemma [26], S. Bachmann [12], J.J. Back [50], S. Baker [55], V. Balagura [7,b], W. Baldini [17], A. Baranov [35], R.J. Barlow [56], S. Barsuk [7], W. Barter [56], F. Baryshnikov [32], V. Batozskaya [29], V. Battista [41], A. Bay [41], J. Beddow [53], F. Bedeschi [24], I. Bediaga [1], A. Beiter [61], L.J. Bel [43], N. Beliy [63], V. Bellee [41], N. Belloli [21,i], K. Belous [37], I. Belyaev [32,40], E. Ben-Haim [8], G. Bencivenni [19], S. Benson [43], S. Beranek [9], A. Berezhnoy [33], R. Bernet [42], D. Berninghoff [12], E. Bertholet [8], A. Bertolin [23],

C. Betancourt [42], F. Betti [15,40], M.O. Bettler [49], M. van Beuzekom [43], Ia. Bezshyiko [42], S. Bifani [47], P. Billoir [8],
A. Birnkraut [10], A. Bizzeti [18,u], M. Bjørn [57], T. Blake [50], F. Blanc [41], S. Blusk [61], V. Bocci [26],
O. Boente Garcia [39], T. Boettcher [58], A. Bondar [36,w], N. Bondar [31], S. Borghi [56,40], M. Borisyak [35],
M. Borsato [39,40], F. Bossu [7], M. Boubdir [9], T.J.V. Bowcock [54], E. Bowen [42], C. Bozzi [17,40], S. Braun [12],
M. Brodski [40], J. Brodzicka [27], D. Brundu [16], E. Buchanan [48], C. Burr [56], A. Bursche [16], J. Buytaert [40],
W. Byczynski [40], S. Cadeddu [16], H. Cai [64], R. Calabrese [17,g], R. Calladine [47], M. Calvi [21,i],
M. Calvo Gomez [38,m], A. Camboni [38,m], P. Campana [19], D.H. Campora Perez [40], L. Capriotti [56],
A. Carbone [15,e], G. Carboni [25], R. Cardinale [20,h], A. Cardini [16], P. Carniti [21,i], L. Carson [52],
K. Carvalho Akiba [2], G. Casse [54], L. Cassina [21], M. Cattaneo [40], G. Cavallero [20,h], R. Cenci [24,p], D. Chamont [7],
M.G. Chapman [48], M. Charles [8], Ph. Charpentier [40], G. Chatzikonstantinidis [47], M. Chefdeville [4], S. Chen [16],
S.-G. Chitic [40], V. Chobanova [39], M. Chrzaszcz [40], A. Chubykin [31], P. Ciambrone [19], X. Cid Vidal [39],
G. Ciezarek [40], P.E.L. Clarke [52], M. Clemencic [40], H.V. Cliff [49], J. Closier [40], V. Coco [40], J. Cogan [6],
E. Cogneras [5], V. Cogoni [16,f], L. Cojocariu [30], P. Collins [40], T. Colombo [40], A. Comerma-Montells [12],
A. Contu [16], G. Coombs [40], S. Coquereau [38], G. Corti [40], M. Corvo [17,g], C.M. Costa Sobral [50], B. Couturier [40],
G.A. Cowan [52], D.C. Craik [58], A. Crocombe [50], M. Cruz Torres [1], R. Currie [52], C. D'Ambrosio [40],
F. Da Cunha Marinho [2], C.L. Da Silva [73], E. Dall'Occo [43], J. Dalseno [48], A. Danilina [32], A. Davis [3],
O. De Aguiar Francisco [40], K. De Bruyn [40], S. De Capua [56], M. De Cian [41], J.M. De Miranda [1], L. De Paula [2],
M. De Serio [14,d], P. De Simone [19], C.T. Dean [53], D. Decamp [4], L. Del Buono [8], B. Delaney [49],
H.-P. Dembinski [11], M. Demmer [10], A. Dendek [28], D. Derkach [35], O. Deschamps [5], F. Dettori [54], B. Dey [65],
A. Di Canto [40], P. Di Nezza [19], S. Didenko [69], H. Dijkstra [40], F. Dordei [40], M. Dorigo [40], A. Dosil Suárez [39],
L. Douglas [53], A. Dovbnya [45], K. Dreimanis [54], L. Dufour [43], G. Dujany [8], P. Durante [40], J.M. Durham [73],
D. Dutta [56], R. Dzhelyadin [37], M. Dziewiecki [12], A. Dziurda [40], A. Dzyuba [31], S. Easo [51], U. Egede [55],
V. Egorychev [32], S. Eidelman [36,w], S. Eisenhardt [52], U. Eitschberger [10], R. Ekelhof [10], L. Eklund [53], S. Ely [61],
A. Ene [30], S. Escher [9], S. Esen [12], H.M. Evans [49], T. Evans [57], A. Falabella [15], N. Farley [47], S. Farry [54],
D. Fazzini [21,40,i], L. Federici [25], G. Fernandez [38], P. Fernandez Declara [40], A. Fernandez Prieto [39],
F. Ferrari [15], L. Ferreira Lopes [41], F. Ferreira Rodrigues [2], M. Ferro-Luzzi [40], S. Filippov [34], R.A. Fini [14],
M. Fiorini [17,g], M. Firlej [28], C. Fitzpatrick [41], T. Fiutowski [28], F. Fleuret [7,b], M. Fontana [16,40],
F. Fontanelli [20,h], R. Forty [40], V. Franco Lima [54], M. Frank [40], C. Frei [40], J. Fu [22,q], W. Funk [40], C. Färber [40],
E. Gabriel [52], A. Gallas Torreira [39], D. Galli [15,e], S. Gallorini [23], S. Gambetta [52], M. Gandelman [2],
P. Gandini [22], Y. Gao [3], L.M. Garcia Martin [71], B. Garcia Plana [39], J. García Pardiñas [42], J. Garra Tico [49],
L. Garrido [38], D. Gascon [38], C. Gaspar [40], L. Gavardi [10], G. Gazzoni [5], D. Gerick [12], E. Gersabeck [56],
M. Gersabeck [56], T. Gershon [50], Ph. Ghez [4], S. Gianì [41], V. Gibson [49], O.G. Girard [41], L. Giubega [30],
K. Gizdov [52], V.V. Gligorov [8], D. Golubkov [32], A. Golutvin [55,69], A. Gomes [1,a], I.V. Gorelov [33], C. Gotti [21,i],
E. Govorkova [43], J.P. Grabowski [12], R. Graciani Diaz [38], L.A. Granado Cardoso [40], E. Graugés [38],
E. Graverini [42], G. Graziani [18], A. Grecu [30], R. Greim [43], P. Griffith [16], L. Grillo [56], L. Gruber [40],
B.R. Gruberg Cazon [57], O. Grünberg [67], E. Gushchin [34], Yu. Guz [37,40], T. Gys [40], C. Göbel [62],
T. Hadavizadeh [57], C. Hadjivasiliou [5], G. Haefeli [41], C. Haen [40], S.C. Haines [49], B. Hamilton [60], X. Han [12],
T.H. Hancock [57], S. Hansmann-Menzemer [12], N. Harnew [57], S.T. Harnew [48], C. Hasse [40], M. Hatch [40],
J. He [63], M. Hecker [55], K. Heinicke [10], A. Heister [9], K. Hennessy [54], L. Henry [71], E. van Herwijnen [40],
M. Heß [67], A. Hicheur [2], D. Hill [57], P.H. Hopchev [41], W. Hu [65], W. Huang [63], Z.C. Huard [59],
W. Hulsbergen [43], T. Humair [55], M. Hushchyn [35], D. Hutchcroft [54], P. Ibis [10], M. Idzik [28], P. Ilten [47],
K. Ivshin [31], R. Jacobsson [40], J. Jalocha [57], E. Jans [43], A. Jawahery [60], F. Jiang [3], M. John [57], D. Johnson [40],
C.R. Jones [49], C. Joram [40], B. Jost [40], N. Jurik [57], S. Kandybei [45], M. Karacson [40], J.M. Kariuki [48], S. Karodia [53],
N. Kazeev [35], M. Kecke [12], F. Keizer [49], M. Kelsey [61], M. Kenzie [49], T. Ketel [44], E. Khairullin [35], B. Khanji [12],
C. Khurewathanakul [41], K.E. Kim [61], T. Kirn [9], S. Klaver [19], K. Klimaszewski [29], T. Klimkovich [11],
S. Koliiev [46], M. Kolpin [12], R. Kopecna [12], P. Koppenburg [43], S. Kotriakhova [31], M. Kozeiha [5], L. Kravchuk [34],
M. Kreps [50], F. Kress [55], P. Krokovny [36,w], W. Krupa [28], W. Krzemien [29], W. Kucewicz [27,l], M. Kucharczyk [27],
V. Kudryavtsev [36,w], A.K. Kuonen [41], T. Kvaratskheliya [32,40], D. Lacarrere [40], G. Lafferty [56], A. Lai [16],
G. Lanfranchi [19], C. Langenbruch [9], T. Latham [50], C. Lazzeroni [47], R. Le Gac [6], A. Leflat [33,40], J. Lefrançois [7],
R. Lefèvre [5], F. Lemaitre [40], O. Leroy [6], T. Lesiak [27], B. Leverington [12], P.-R. Li [63], T. Li [3], Z. Li [61], X. Liang [61],
T. Likhomanenko [68], R. Lindner [40], F. Lionetto [42], V. Lisovskyi [7], X. Liu [3], D. Loh [50], A. Loi [16], I. Longstaff [53],
J.H. Lopes [2], D. Lucchesi [23,o], M. Lucio Martinez [39], A. Lupato [23], E. Luppi [17,g], O. Lupton [40], A. Lusiani [24],

X. Lyu [63], F. Machefert [7], F. Maciuc [30], V. Macko [41], P. Mackowiak [10], S. Maddrell-Mander [48], O. Maev [31,40], K. Maguire [56], D. Maisuzenko [31], M.W. Majewski [28], S. Malde [57], B. Malecki [27], A. Malinin [68], T. Maltsev [36,w], G. Manca [16,f], G. Mancinelli [6], D. Marangotto [22,q], J. Maratas [5,v], J.F. Marchand [4], U. Marconi [15], C. Marin Benito [38], M. Marinangeli [41], P. Marino [41], J. Marks [12], G. Martellotti [26], M. Martin [6], M. Martinelli [41], D. Martinez Santos [39], F. Martinez Vidal [71], A. Massafferri [1], R. Matev [40], A. Mathad [50], Z. Mathe [40], C. Matteuzzi [21], A. Mauri [42], E. Maurice [7,b], B. Maurin [41], A. Mazurov [47], M. McCann [55,40], A. McNab [56], R. McNulty [13], J.V. Mead [54], B. Meadows [59], C. Meaux [6], F. Meier [10], N. Meinert [67], D. Melnychuk [29], M. Merk [43], A. Merli [22,q], E. Michielin [23], D.A. Milanes [66], E. Millard [50], M.-N. Minard [4], L. Minzoni [17,g], D.S. Mitzel [12], A. Mogini [8], J. Molina Rodriguez [1,y], T. Mombächer [10], I.A. Monroy [66], S. Monteil [5], M. Morandin [23], G. Morello [19], M.J. Morello [24,t], O. Morgunova [68], J. Moron [28], A.B. Morris [6], R. Mountain [61], F. Muheim [52], M. Mulder [43], D. Müller [40], J. Müller [10], K. Müller [42], V. Müller [10], P. Naik [48], T. Nakada [41], R. Nandakumar [51], A. Nandi [57], I. Nasteva [2], M. Needham [52], N. Neri [22], S. Neubert [12], N. Neufeld [40], M. Neuner [12], T.D. Nguyen [41], C. Nguyen-Mau [41,n], S. Nieswand [9], R. Niet [10], N. Nikitin [33], A. Nogay [68], D.P. O'Hanlon [15], A. Oblakowska-Mucha [28], V. Obraztsov [37], S. Ogilvy [19], R. Oldeman [16,f], C.J.G. Onderwater [72], A. Ossowska [27], J.M. Otalora Goicochea [2], P. Owen [42], A. Oyanguren [71], P.R. Pais [41], A. Palano [14], M. Palutan [19,40], G. Panshin [70], A. Papanestis [51], M. Pappagallo [52], L.L. Pappalardo [17,g], W. Parker [60], C. Parkes [56], G. Passaleva [18,40], A. Pastore [14], M. Patel [55], C. Patrignani [15,e], A. Pearce [40], A. Pellegrino [43], G. Penso [26], M. Pepe Altarelli [40], S. Perazzini [40], D. Pereima [32], P. Perret [5], L. Pescatore [41], K. Petridis [48], A. Petrolini [20,h], A. Petrov [68], M. Petruzzo [22,q], B. Pietrzyk [4], G. Pietrzyk [41], M. Pikies [27], D. Pinci [26], F. Pisani [40], A. Pistone [20,h], A. Piucci [12], V. Placinta [30], S. Playfer [52], M. Plo Casasus [39], F. Polci [8], M. Poli Lener [19], A. Poluektov [50], N. Polukhina [69], I. Polyakov [61], E. Polycarpo [2], G.J. Pomery [48], S. Ponce [40], A. Popov [37], D. Popov [11,40], S. Poslavskii [37], C. Potterat [2], E. Price [48], J. Prisciandaro [39], C. Prouve [48], V. Pugatch [46], A. Puig Navarro [42], H. Pullen [57], G. Punzi [24,p], W. Qian [63], J. Qin [63], R. Quagliani [8], B. Quintana [5], B. Rachwal [28], J.H. Rademacker [48], M. Rama [24], M. Ramos Pernas [39], M.S. Rangel [2], F. Ratnikov [35,x], G. Raven [44], M. Ravonel Salzgeber [40], M. Reboud [4], F. Redi [41], S. Reichert [10], A.C. dos Reis [1], C. Remon Alepuz [71], V. Renaudin [7], S. Ricciardi [51], S. Richards [48], K. Rinnert [54], P. Robbe [7], A. Robert [8], A.B. Rodrigues [41], E. Rodrigues [59], J.A. Rodriguez Lopez [66], A. Rogozhnikov [35], S. Roiser [40], A. Rollings [57], V. Romanovskiy [37], A. Romero Vidal [39,40], M. Rotondo [19], M.S. Rudolph [61], T. Ruf [40], J. Ruiz Vidal [71], J.J. Saborido Silva [39], N. Sagidova [31], B. Saitta [16,f], V. Salustino Guimaraes [62], C. Sanchez Mayordomo [71], B. Sanmartin Sedes [39], R. Santacesaria [26], C. Santamarina Rios [39], M. Santimaria [19], E. Santovetti [25,j], G. Sarpis [56], A. Sarti [19,k], C. Satriano [26,s], A. Satta [25], D.M. Saunders [48], D. Savrina [32,33], S. Schael [9], M. Schellenberg [10], M. Schiller [53], H. Schindler [40], M. Schmelling [11], T. Schmelzer [10], B. Schmidt [40], O. Schneider [41], A. Schopper [40], H.F. Schreiner [59], M. Schubiger [41], M.H. Schune [7,40], R. Schwemmer [40], B. Sciascia [19], A. Sciubba [26,k], A. Semennikov [32], E.S. Sepulveda [8], A. Sergi [47,40], N. Serra [42], J. Serrano [6], L. Sestini [23], P. Seyfert [40], M. Shapkin [37], Y. Shcheglov [31,†], T. Shears [54], L. Shekhtman [36,w], V. Shevchenko [68], B.G. Siddi [17], R. Silva Coutinho [42], L. Silva de Oliveira [2], G. Simi [23,o], S. Simone [14,d], N. Skidmore [12], T. Skwarnicki [61], I.T. Smith [52], M. Smith [55], l. Soares Lavra [1], M.D. Sokoloff [59], F.J.P. Soler [53], B. Souza De Paula [2], B. Spaan [10], P. Spradlin [53], F. Stagni [40], M. Stahl [12], S. Stahl [40], P. Stefko [41], S. Stefkova [55], O. Steinkamp [42], S. Stemmle [12], O. Stenyakin [37], M. Stepanova [31], H. Stevens [10], S. Stone [61], B. Storaci [42], S. Stracka [24,p], M.E. Stramaglia [41], M. Straticiuc [30], U. Straumann [42], S. Strokov [70], J. Sun [3], L. Sun [64], K. Swientek [28], V. Syropoulos [44], T. Szumlak [28], M. Szymanski [63], S. T'Jampens [4], Z. Tang [3], A. Tayduganov [6], T. Tekampe [10], G. Tellarini [17], F. Teubert [40], E. Thomas [40], J. van Tilburg [43], M.J. Tilley [55], V. Tisserand [5], M. Tobin [41], S. Tolk [40], L. Tomassetti [17,g], D. Tonelli [24], R. Tourinho Jadallah Aoude [1], E. Tournefier [4], M. Traill [53], M.T. Tran [41], M. Tresch [42], A. Trisovic [49], A. Tsaregorodtsev [6], A. Tully [49], N. Tuning [43,40], A. Ukleja [29], A. Usachov [7], A. Ustyuzhanin [35], U. Uwer [12], C. Vacca [16,f], A. Vagner [70], V. Vagnoni [15], A. Valassi [40], S. Valat [40], G. Valenti [15], R. Vazquez Gomez [40], P. Vazquez Regueiro [39], S. Vecchi [17], M. van Veghel [43], J.J. Velthuis [48], M. Veltri [18,r], G. Veneziano [57], A. Venkateswaran [61], T.A. Verlage [9], M. Vernet [5], M. Vesterinen [57], J.V. Viana Barbosa [40], D. Vieira [63], M. Vieites Diaz [39], H. Viemann [67], X. Vilasis-Cardona [38,m], A. Vitkovskiy [43], M. Vitti [49], V. Volkov [33], A. Vollhardt [42], B. Voneki [40], A. Vorobyev [31], V. Vorobyev [36,w], C. Voß [9], J.A. de Vries [43], C. Vázquez Sierra [43], R. Waldi [67], J. Walsh [24], J. Wang [61], M. Wang [3,*], Y. Wang [65], Z. Wang [42], D.R. Ward [49], H.M. Wark [54], N.K. Watson [47],

D. Websdale [55], A. Weiden [42], C. Weisser [58], M. Whitehead [9], J. Wicht [50], G. Wilkinson [57], M. Wilkinson [61], M.R.J. Williams [56], M. Williams [58], T. Williams [47], F.F. Wilson [51,40], J. Wimberley [60], M. Winn [7], J. Wishahi [10], W. Wislicki [29], M. Witek [27], G. Wormser [7], S.A. Wotton [49], K. Wyllie [40], D. Xiao [65], Y. Xie [65], A. Xu [3], M. Xu [65], Q. Xu [63], Z. Xu [3], Z. Xu [4], Z. Yang [3], Z. Yang [60], Y. Yao [61], H. Yin [65], J. Yu [65], X. Yuan [61], O. Yushchenko [37], K.A. Zarebski [47], M. Zavertyaev [11,c], L. Zhang [3], Y. Zhang [7], A. Zhelezov [12], Y. Zheng [63], X. Zhu [3], V. Zhukov [9,33], J.B. Zonneveld [52], S. Zucchelli [15]

[1] *Centro Brasileiro de Pesquisas Físicas (CBPF), Rio de Janeiro, Brazil*
[2] *Universidade Federal do Rio de Janeiro (UFRJ), Rio de Janeiro, Brazil*
[3] *Center for High Energy Physics, Tsinghua University, Beijing, China*
[4] *Univ. Grenoble Alpes, Univ. Savoie Mont Blanc, CNRS, IN2P3-LAPP, Annecy, France*
[5] *Clermont Université, Université Blaise Pascal, CNRS/IN2P3, LPC, Clermont-Ferrand, France*
[6] *Aix Marseille Univ, CNRS/IN2P3, CPPM, Marseille, France*
[7] *LAL, Univ. Paris-Sud, CNRS/IN2P3, Université Paris-Saclay, Orsay, France*
[8] *LPNHE, Université Pierre et Marie Curie, Université Paris Diderot, CNRS/IN2P3, Paris, France*
[9] *I. Physikalisches Institut, RWTH Aachen University, Aachen, Germany*
[10] *Fakultät Physik, Technische Universität Dortmund, Dortmund, Germany*
[11] *Max-Planck-Institut für Kernphysik (MPIK), Heidelberg, Germany*
[12] *Physikalisches Institut, Ruprecht-Karls-Universität Heidelberg, Heidelberg, Germany*
[13] *School of Physics, University College Dublin, Dublin, Ireland*
[14] *Sezione INFN di Bari, Bari, Italy*
[15] *Sezione INFN di Bologna, Bologna, Italy*
[16] *Sezione INFN di Cagliari, Cagliari, Italy*
[17] *Sezione INFN di Ferrara, Ferrara, Italy*
[18] *Sezione INFN di Firenze, Firenze, Italy*
[19] *Laboratori Nazionali dell'INFN di Frascati, Frascati, Italy*
[20] *Sezione INFN di Genova, Genova, Italy*
[21] *Sezione INFN di Milano Bicocca, Milano, Italy*
[22] *Sezione INFN di Milano, Milano, Italy*
[23] *Sezione INFN di Padova, Padova, Italy*
[24] *Sezione INFN di Pisa, Pisa, Italy*
[25] *Sezione INFN di Roma Tor Vergata, Roma, Italy*
[26] *Sezione INFN di Roma La Sapienza, Roma, Italy*
[27] *Henryk Niewodniczanski Institute of Nuclear Physics Polish Academy of Sciences, Kraków, Poland*
[28] *AGH - University of Science and Technology, Faculty of Physics and Applied Computer Science, Kraków, Poland*
[29] *National Center for Nuclear Research (NCBJ), Warsaw, Poland*
[30] *Horia Hulubei National Institute of Physics and Nuclear Engineering, Bucharest-Magurele, Romania*
[31] *Petersburg Nuclear Physics Institute (PNPI), Gatchina, Russia*
[32] *Institute of Theoretical and Experimental Physics (ITEP), Moscow, Russia*
[33] *Institute of Nuclear Physics, Moscow State University (SINP MSU), Moscow, Russia*
[34] *Institute for Nuclear Research of the Russian Academy of Sciences (INR RAS), Moscow, Russia*
[35] *Yandex School of Data Analysis, Moscow, Russia*
[36] *Budker Institute of Nuclear Physics (SB RAS), Novosibirsk, Russia*
[37] *Institute for High Energy Physics (IHEP), Protvino, Russia*
[38] *ICCUB, Universitat de Barcelona, Barcelona, Spain*
[39] *Instituto Galego de Física de Altas Enerxías (IGFAE), Universidade de Santiago de Compostela, Santiago de Compostela, Spain*
[40] *European Organization for Nuclear Research (CERN), Geneva, Switzerland*
[41] *Institute of Physics, Ecole Polytechnique Fédérale de Lausanne (EPFL), Lausanne, Switzerland*
[42] *Physik-Institut, Universität Zürich, Zürich, Switzerland*
[43] *Nikhef National Institute for Subatomic Physics, Amsterdam, the Netherlands*
[44] *Nikhef National Institute for Subatomic Physics and VU University Amsterdam, Amsterdam, the Netherlands*
[45] *NSC Kharkiv Institute of Physics and Technology (NSC KIPT), Kharkiv, Ukraine*
[46] *Institute for Nuclear Research of the National Academy of Sciences (KINR), Kyiv, Ukraine*
[47] *University of Birmingham, Birmingham, United Kingdom*
[48] *H.H. Wills Physics Laboratory, University of Bristol, Bristol, United Kingdom*
[49] *Cavendish Laboratory, University of Cambridge, Cambridge, United Kingdom*
[50] *Department of Physics, University of Warwick, Coventry, United Kingdom*
[51] *STFC Rutherford Appleton Laboratory, Didcot, United Kingdom*
[52] *School of Physics and Astronomy, University of Edinburgh, Edinburgh, United Kingdom*
[53] *School of Physics and Astronomy, University of Glasgow, Glasgow, United Kingdom*
[54] *Oliver Lodge Laboratory, University of Liverpool, Liverpool, United Kingdom*
[55] *Imperial College London, London, United Kingdom*
[56] *School of Physics and Astronomy, University of Manchester, Manchester, United Kingdom*
[57] *Department of Physics, University of Oxford, Oxford, United Kingdom*
[58] *Massachusetts Institute of Technology, Cambridge, MA, United States*
[59] *University of Cincinnati, Cincinnati, OH, United States*
[60] *University of Maryland, College Park, MD, United States*
[61] *Syracuse University, Syracuse, NY, United States*
[62] *Pontifícia Universidade Católica do Rio de Janeiro (PUC-Rio), Rio de Janeiro, Brazil, associated to [2]*
[63] *University of Chinese Academy of Sciences, Beijing, China, associated to [3]*
[64] *School of Physics and Technology, Wuhan University, Wuhan, China, associated to [3]*
[65] *Institute of Particle Physics, Central China Normal University, Wuhan, Hubei, China, associated to [3]*
[66] *Departamento de Fisica, Universidad Nacional de Colombia, Bogota, Colombia, associated to [8]*
[67] *Institut für Physik, Universität Rostock, Rostock, Germany, associated to [12]*
[68] *National Research Centre Kurchatov Institute, Moscow, Russia, associated to [32]*
[69] *National University of Science and Technology MISIS, Moscow, Russia, associated to [32]*

[70] *National Research Tomsk Polytechnic University, Tomsk, Russia, associated to* [32]
[71] *Instituto de Fisica Corpuscular, Centro Mixto Universidad de Valencia - CSIC, Valencia, Spain, associated to* [38]
[72] *Van Swinderen Institute, University of Groningen, Groningen, the Netherlands, associated to* [43]
[73] *Los Alamos National Laboratory (LANL), Los Alamos, United States, associated to* [61]

[*] Corresponding author.
     E-mail address: mengzhen.wang@cern.ch (M. Wang).
[a] Universidade Federal do Triângulo Mineiro (UFTM), Uberaba-MG, Brazil.
[b] Laboratoire Leprince-Ringuet, Palaiseau, France.
[c] P.N. Lebedev Physical Institute, Russian Academy of Science (LPI RAS), Moscow, Russia.
[d] Università di Bari, Bari, Italy.
[e] Università di Bologna, Bologna, Italy.
[f] Università di Cagliari, Cagliari, Italy.
[g] Università di Ferrara, Ferrara, Italy.
[h] Università di Genova, Genova, Italy.
[i] Università di Milano Bicocca, Milano, Italy.
[j] Università di Roma Tor Vergata, Roma, Italy.
[k] Università di Roma La Sapienza, Roma, Italy.
[l] AGH - University of Science and Technology, Faculty of Computer Science, Electronics and Telecommunications, Kraków, Poland.
[m] LIFAELS, La Salle, Universitat Ramon Llull, Barcelona, Spain.
[n] Hanoi University of Science, Hanoi, Vietnam.
[o] Università di Padova, Padova, Italy.
[p] Università di Pisa, Pisa, Italy.
[q] Università degli Studi di Milano, Milano, Italy.
[r] Università di Urbino, Urbino, Italy.
[s] Università della Basilicata, Potenza, Italy.
[t] Scuola Normale Superiore, Pisa, Italy.
[u] Università di Modena e Reggio Emilia, Modena, Italy.
[v] Iligan Institute of Technology (IIT), Iligan, Philippines.
[w] Novosibirsk State University, Novosibirsk, Russia.
[x] National Research University Higher School of Economics, Moscow, Russia.
[y] Escuela Agrícola Panamericana, San Antonio de Oriente, Honduras.
[†] Deceased.